

**SYNTHESIS AND CHARACTERIZATION OF HEMATITE (α -Fe₂O₃)
NANOPARTICLES**



Kitibodee Supattarasakda

A Thesis Submitted in Partial Fulfilment of the Requirements
for the Degree of Master of Science
The Petroleum and Petrochemical College, Chulalongkorn University
in Academic Partnership with
The University of Michigan, The University of Oklahoma,
and Case Western Reserve University

2012


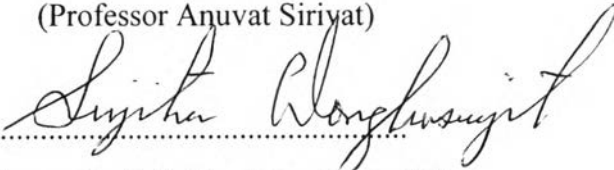
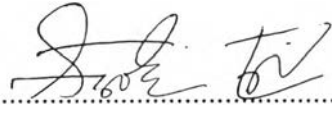
I28374320

Thesis Title: Synthesis and Characterization of Hematite (α -Fe₂O₃)
Nanoparticles
By: Kitibodee Supattarasakda
Program: Polymer Science
Thesis Advisor: Professor Anuvat Sirivat

Accepted by the Petroleum and Petrochemical College, Chulalongkorn University, in partial fulfilment of the requirements for the Degree of Master of Science.


..... College Dean
(Asst. Prof. Pomthong Malakul)

Thesis Committee:


.....
(Professor Anuvat Sirivat)

.....
(Assoc. Prof. Sujitra Wongkasemjit)

.....
(Asst. Prof. Wanchai Lerdwijitjarud)

ABSTRACT

5372008063: Polymer Science Program

Kitibodee Supattarasakda: Synthesis and Characterization of Hematite (α -Fe₂O₃) Nanoparticles.

Thesis Advisor: Professor Anuvat Sirivat 146 pp.

Keywords: Size-controlled hematite (α -Fe₂O₃)/ Magnetic nanoparticles/ Chemical precipitation method/ Superparamagnetic behavior

Hematite (α -Fe₂O₃) nanoparticles were successfully synthesized from 2-line ferrihydrite precursor via a simple chemical precipitation method by using sodium hydroxide as a precipitating agent, with trace amounts of Fe (II) as a catalyst, and under nitrogen atmosphere. The influences of the synthesis conditions, such as the precursor concentration, the solution pH, the amount of catalyst on the size and morphology of the hematite particles were systematically investigated. The structure and morphology of the synthesized hematite particles were characterized by XRD, FT-IR, TG/DTA, and FE-SEM. Moreover, the electrical and magnetic properties were studied by using an electrometer with a custom-built two-point probe and a vibrating sample magnetometer (VSM), respectively. The results indicate that the synthesized products fabricated at pH 5-9 and at temperatures between 60-100 °C for 1h are of a single phase of the hexagonal structure hematite without any other impurities. The physical morphology of the synthesized hematite appears to be composed of a large number of very small particles which can be called as the “raspberry shape”. Particle size and shape of the synthesized hematite can be easily controlled by adjusting the synthesis conditions. The particle size of the synthesized hematite can be successfully controlled to be in the range of 50-150 nm. Different morphologies consisting of the spherical-like, the cubic-like, and the ellipsoidal particles are also obtained by using the present synthesis method. Different particle sizes and shapes of the synthesized hematite are shown to critically affect the electrical and magnetic properties.

บทคัดย่อ

กิตติบดียุทธศาสตร์ : การสังเคราะห์และพิสูจน์เอกลักษณ์ของอนุภาคนาโนเมตรเฮมาไทต์ (Synthesis and Characterization of Hematite (α -Fe₂O₃) Nanoparticles) อ. ที่ปรึกษา : ศ.ดร. อนุวัฒน์ ศิริวัฒน์ 146 หน้า

อนุภาคนาโนเมตรเฮมาไทต์ (α -Fe₂O₃) สามารถสังเคราะห์ได้โดยวิธีตกตะกอนทางเคมีแบบง่าย (Simple chemical precipitation method) จากสารเริ่มต้นเฟอร์ริไฮไดรด์ (2-line ferrihydrite) โดยใช้โซเดียมไฮดรอกไซด์ (NaOH) เป็นสารตกตะกอน และใช้เฟอร์ริสไออน (Fe(II)) เป็นสารเร่งปฏิกิริยา ภายใต้สภาวะบรรยากาศของก๊าซไนโตรเจน อิทธิพลของสภาวะการสังเคราะห์ เช่น ความเข้มข้นของสารเริ่มต้น, ความเป็นกรด-เบสของสารละลาย, ปริมาณของสารเร่งปฏิกิริยา ต่อขนาดและสัณฐานวิทยาของอนุภาคเฮมาไทต์ถูกศึกษาอย่างเป็นระบบ โดยโครงสร้างและสัณฐานวิทยาของอนุภาคเฮมาไทต์ถูกพิสูจน์เอกลักษณ์โดยใช้เครื่อง XRD, FT-IR, TG/DTA, และ FE-SEM ยิ่งกว่านั้น สมบัติทางไฟฟ้าและสมบัติแม่เหล็กยังถูกศึกษาโดยใช้เครื่องวัดสมบัติทางไฟฟ้าแบบสองโพรบที่สร้างขึ้นเอง (Electrometer with a custom-built two-point probe) และเครื่องวัดสมบัติแม่เหล็กแบบสั่นตัวอย่าง (Vibrating sample magnetometer), ตามลำดับ ผลการทดลองบ่งชี้ให้เห็นว่าผลิตภัณฑ์ที่สังเคราะห์ได้ที่สภาวะความเป็นกรด-เบสระหว่าง pH 5-9 และ ที่อุณหภูมิระหว่าง 60-100 °C เป็นเวลา 1 ชั่วโมง เป็นเฟสเดียวของโครงสร้างหกเหลี่ยม (Single phase of hexagonal structure) ของเฮมาไทต์โดยปราศจากสิ่งเจือปนอื่นๆ โครงสร้างทางกายภาพของเฮมาไทต์ที่สังเคราะห์ได้ประกอบด้วยอนุภาคนาโนขนาดเล็กเป็นจำนวนมาก ซึ่งสามารถเรียกโครงสร้างดังกล่าวว่า “รูปร่างแบบราสเบอร์รี่ (Raspberry shape)” ขนาดและรูปร่างของเฮมาไทต์สามารถควบคุมได้ง่ายๆ โดยการปรับสภาวะการสังเคราะห์ โดยขนาดอนุภาคของเฮมาไทต์ที่สามารถควบคุมให้อยู่ในช่วง 50-150 นาโนเมตร ส่วนสัณฐานวิทยาที่แตกต่างกันประกอบด้วย รูปร่างคล้ายทรงกลม (Spherical-like), รูปร่างคล้ายลูกบาศก์ (Cubic-like), และรูปร่างทรงรี (Ellipsoidal) สามารถสังเคราะห์ได้โดยวิธีการสังเคราะห์นี้เช่นกัน การที่อนุภาคเฮมาไทต์มีขนาดและรูปร่างที่แตกต่างกัน ส่งผลต่อสมบัติทางไฟฟ้าและสมบัติแม่เหล็กของอนุภาคเฮมาไทต์ที่ได้อย่างมาก

ACKNOWLEDGEMENTS

I would like to express my sincere gratitude to all those who gave the possibility to complete this thesis work.

First of all, I am grateful for the scholarship and funding of the thesis work provided by the Petroleum and Petrochemical College, and by the Center of Excellence on Petrochemical, and Materials Technology, Thailand.

I am deeply indebted to my thesis advisors, Professor Anuvat Sirivat who gave admirable guidance, encouragement, stimulating suggestions and helped me in all the time of my research.

My sincere thank are due to the official committees, Assoc. Prof. Sujitra Wongkasemjit and Asst. Prof. Wanchai Lerdwijitjarud, for their detailed review, constructive criticism and excellent advices.

I would like to thank Asst. Prof. Pongsakorn Jantaratana, Department of Physics, Faculty of Science, Kasetsart University for the magnetic properties measurement and for helpful knowledge of theory and concept used. I also would like to show my appreciation to all special senior students in the AS group; especially, to Ms. Karat Petcharoen and Ms. Nophawan Paradee for their helpful suggestions.

Lastly, this special thesis would not have been possible without the knowledge received from all the lecturers and staffs at the Petroleum and Petrochemical College, plus love and constant support from my family and friends.

TABLE OF CONTENTS

	PAGE
Title Page	i
Abstract (in English)	iii
Abstract (in Thai)	iv
Acknowledgements	v
Table of Contents	vi
List of Tables	ix
List of Figures	x
Abbreviations	xii
List of Symbols	xiii
 CHAPTER	
I INTRODUCTION	1
 II THEORETICAL BACKGROUND AND LITERATURE	
REVIEW	3
2.1 Magnetic Nanoparticles	3
2.1.1 Iron Oxides	3
2.1.2 Iron(III) Oxides	4
2.1.3 Iron Oxide Nanoparticles	7
2.2 Magnetic Behaviors	8
2.2.1 Type of Magnetisms	8
2.2.2 Hysteresis Curve of Ferromagnetic Materials	11
2.2.3 Superparamagnetic Behavior	14
2.3 Applications of Magnetic Nanoparticles	15
2.4 Literature Review	18
2.4.1 Synthesis of Hematite Nanoparticles	18
2.4.2 Nucleation and Crystal Growth	22
2.4.3 Catalytic Phase Transformation Mechanisms	24
2.4.4 Factors Affecting the Particle Size of Hematite	25

CHAPTER		PAGE
III	METHODOLOGY	29
	3.1 Materials	29
	3.1.1 Chemicals	29
	3.1.2 Solvent	29
	3.1.3 Gas	29
	3.2 Equipment	29
	3.2.1 Analytical Instruments	29
	3.2.2 Glassware and Aparatus	30
	3.3 Experimental	30
	3.3.1 Synthesis of Hematite Nanoparticles	30
	3.3.2 Particle Size and Morphology Control	31
	3.4 Characterization and Measurement	32
	3.4.1 Characteristics of Hematite Nanoparticles	32
	3.4.2 Particle Size and Morphology of Hematite Nanoparticles	33
	3.4.3 Properties of Hematite Nanoparticles	34
IV	SYNTHESIS AND CHARACTERIZATION OF SIZE- CONTROLLED HEMATITE (α-Fe₂O₃) NANOPARTICLES VIA THE CHEMICAL PRECIPITATION METHOD	36
	4.1 Abstract	37
	4.2 Introduction	38
	4.3 Experimental	39
	4.4 Results and Discussion	42
	4.5 Conclusions	50
	4.6 Acknowledgements	51
	4.7 References	51

CHAPTER		PAGE
V	CONCLUSIONS AND RECOMMENDATIONS	61
	5.1 Conclusions	61
	5.2 Recommendations	62
	REFERENCES	63
	APPENDICES	69
	Appendix A Amounts of Chemicals Used to Synthesize Hematite Particles and Yield Percentage of the Products	69
	Appendix B XRD Patterns of the Synthesized Hematite Nanoparticles	73
	Appendix C FT-IR Spectra of the Synthesized Hematite Nanoparticles	79
	Appendix D TG/DTA Curves of the Synthesized Hematite Nanoparticles	82
	Appendix E FE-SEM Images of the Synthesized Hematite Nanoparticles	84
	Appendix F Particle Sizes and Particle Size Distributions of the Synthesized Hematite Nanoparticles	98
	Appendix G Specific Surface Area Measurement of the Synthesized Hematite Nanoparticles	119
	Appendix H Electrical Conductivity Measurement of the Synthesized Hematite Nanoparticles	121
	Appendix I Magnetic Properties Measurement of the Synthesized Hematite Nanoparticles	142
	CURRICULUM VITAE	146

LIST OF TABLES

TABLE		PAGE
CHAPTER II		
2.1	The sixteen iron oxides	3
2.2	Physical and magnetic properties of the iron oxides	6
2.3	Comparison of the synthesis methods for hematite nanoparticles	22
2.4	Summary of Fe(II) ion forms existed at different pHs	26
2.5	Transformation conditions from ferrihydrite to various iron (hydr)oxides	28
CHAPTER IV		
4.1	Summary of the magnetic parameters of the synthesized hematite nanoparticles with different particle sizes and morphologies	56

LIST OF FIGURES

FIGURE		PAGE
CHAPTER II		
2.1	Graphical representations of the fundamental crystal structures of Fe_2O_3 : (a) $\alpha\text{-Fe}_2\text{O}_3$; (b) $\beta\text{-Fe}_2\text{O}_3$; (c) $\gamma\text{-Fe}_2\text{O}_3$; and (d) $\varepsilon\text{-Fe}_2\text{O}_3$.	4
2.2	Crystal structures of: (a) hematite; and (b) magnetite & maghemite.	7
2.3	Magnetic dipole moments of paramagnetic materials.	9
2.4	Magnetic dipole moments of ferromagnetic materials.	9
2.5	Magnetic dipole moments of antiferromagnetic materials.	10
2.6	Magnetic dipole moments of ferrimagnetic materials.	10
2.7	Development of magnetism in magnetic materials.	11
2.8	Hysteresis curve of ferromagnetic materials.	12
2.9	Hysteresis curves of: (a) hard; and (b) soft magnetic materials.	13
2.10	Schematic representation of: (a) magnetization behavior of ferromagnetic and superparamagnetic NPs; and (b) relationship between NP size and the magnetic domain structures.	14
2.11	Magnetization curve of superparamagnetic materials.	15
2.12	Diagrammatic sketch of the solid-state transformation mechanism of hematite.	24
2.13	Diagrammatic sketch of the dissolution/reprecipitation mechanism of hematite.	25
CHAPTER III		
3.1	Experimental setup of the chemical precipitation method.	31

FIGURE	PAGE
CHAPTER IV	
4.1 XRD patterns of the 2-line ferrihydrite precursor ($C = 0.3$ M, pH 7) and the synthesized hematite nanoparticles ($C = 0.3$ M, $n_{\text{Fe(II)}}/n_{\text{Fe(III)}} = 0.02$, pH 7, 100 °C, and 1h).	56
4.2 FT-IR spectra of the 2-line ferrihydrite precursor ($C = 0.3$ M, pH 7) and the synthesized hematite nanoparticles ($C = 0.3$ M, $n_{\text{Fe(II)}}/n_{\text{Fe(III)}} = 0.02$, pH 7, 100 °C, and 1h).	57
4.3 TG-DTA curves of the synthesized hematite nanoparticles ($C = 0.3$ M, $n_{\text{Fe(II)}}/n_{\text{Fe(III)}} = 0.02$, pH 7, 100 °C, and 1h).	57
4.4 Average particle sizes of the synthesized hematite nanoparticles under the effect of various preparation conditions: (a) the precursor concentration; (b) the solution pH; (c) the amount of Fe(II); and (d) the ionic strength.	58
4.5 FE-SEM images of: (a) the 2-line ferrihydrite precursor ($C = 0.3$ M, pH 7); and the synthesized hematite nanoparticles ($n_{\text{Fe(II)}}/n_{\text{Fe(III)}} = 0.02$, pH 7, 100 °C, and 1h); (b) hematite $C = 0.1$ M; (c) hematite $C = 0.3$ M; and (d) hematite $C = 0.5$ M (Note: <i>inset plots</i> demonstrate the particle size distribution from the corresponding FE-SEM images).	58
4.6 FE-SEM images of the synthesized hematite nanoparticles with different morphologies: (a, b) the spherical-like particles at low and high magnifications; (c) the cubic-like particles; and (d) the ellipsoidal particles (Note: <i>inset</i> in (b) represents the magnified view of the particle surface).	59
4.7 Specific conductivities of the synthesized hematite nanoparticles with different particle sizes and morphologies.	59
4.8 Room temperature magnetization curves of the synthesized hematite nanoparticles with: (a) different particle sizes; and (b) different morphologies (Note: <i>inset plots</i> illustrate the magnified view of the corresponding magnetization curves).	60

ABBREVIATIONS

XRD	X-Ray Diffractometer
FT-IR	Fourier Transform Infrared Spectrometer
TG/DTA	Thermogravimetric/Differential Thermal Analyzer
FE-SEM	Field-Emission Scanning Electron Microscope
BET	Brunauer-Emmett-Teller
VSM	Vibrating Sample Magnetometer
ccp	cubic closed packing
hcp	hexagonal closed packing
NPs	Nanoparticles
MRI	Magnetic Resonance Imaging
pzc	point of zero charge
w/o	water in oil
D/R	Dissolution/Reprecipitation
S-ST	Solid-State Transformation
FWHM	Full width at half maximum
SD	Standard deviation
JCPDS	Joint Committee on Powder Diffraction Standard
PDI	Polydispersity Index
SSA	Specific surface area

LIST OF SYMBOLS

C	precursor concentration (M)
I	ionic strength (mol/L)
C_i	molar concentration of each individual ion in the solution (mol/L)
Z_i	valence of each individual ion in the solution (-)
$n_{\text{Fe(II)}}/n_{\text{Fe(III)}}$	molar ratio of Fe(II) to Fe(III) (-)
H	applied magnetic field (Oe)
H_c	coercive force (Oe)
M	magnetization (emu/g)
M_r	remanence magnetization (at $H = 0$ Oe) (emu/g)
M_s	saturation (maximum) magnetization (emu/g)
D	crystallite size (nm)
k	grain shape dependent constant (-)
λ	wave length of X-ray beam (nm)
β	full width at half maximum (FWHM) (rad)
θ	diffraction angle ($^\circ$)
$D[p,q]$	general form of the mean diameter
n_i	number of the i^{th} particle
D_i	diameter of i^{th} particle
$(p-q)$	algebraic power of $D[p,q]$
D_n	number mean diameter or $D[1,0]$
D_v	volume mean diameter or $D[4,3]$
D_s	surface mean diameter or $D[3,2]$
σ	specific conductivity (S/cm)
ρ	specific resistivity ($\Omega\cdot\text{cm}$)
R_s	sheet resistivity (Ω)
R	resistance (Ω)
I	resultant current (A)
K	geometric correction factor (-)
V	applied voltage (V)
t	thickness of the disc sample(cm)